Received: May 18, 2020
Revised: June 30, 2020
Accepted: June 30, 2020

Effect of activated carbon on their performance as HT catalyst supports for fermentative hydrogen production

Pornthip Wimonsong[1,*] and Rachnarin Nitisoravut[2]

[1]*Department of Disaster Management, Faculty of Science and Technology, Suratthani Rajabhat University, Suratthani 84100, Thailand*

[2]*School of Bio-Chemical Engineering and Technology, Sirindhorn International Institute of Technology, Thammasat University, Pathumthani 12121, Thailand*

Abstract

The activities of modified hydrotalcite with Ni and Zn catalysts supported on treated activated carbon (Ni-HT/TAC and Zn-HT/TAC) were investigated for their potential enhancement of fermentative hydrogen production. The experiments were performed under batch tests using sucrose-fed anaerobic mixed culture at 37 °C. The hybrid catalysts of Ni-HT/TAC and Zn-HT/TAC were synthesized by incipient impregnation methods. The X-ray powder diffraction patterns exhibit the characteristic diffractions of HT, indicating that the HTs were successfully coated onto TAC. The difference in dose of Ni-HT/TAC and Zn-HT/TAC showed a significant difference in hydrogen production over the studied range of 0.00-16.67 g/L. The maximum hydrogen yields obtained at 8.33 g/L of Ni-HT/TAC and Zn-HT/TAC were 2.66 and 3.08 mol H_2/mol sucrose with 9.29% and 26.62% increment as compared to the control, respectively. In addition, the effect of modified hydrotalcite with Ni and Zn catalysts loading on TAC for fermentative hydrogen production were studied. The hydrogen production profiles showed that the initial activity of the Ni-HT/TAC catalyst at 24 h was more active than Zn-HT/TAC catalyst. On the contrary, after 120 h, the activity of the Zn-HT/TAC catalyst was more stable than Ni-HT/TAC catalyst. The maximum cumulative hydrogen production was obtained from Zn-HT/TAC with a 7.53% increment as compared to TAC. On the other hand, Ni-HT/TAC showed a decrease in the maximum cumulative hydrogen production with 7.18% as compared to TAC. Therefore, TAC showed the potential as modified HT catalyst supports, especially Zn metal for fermentative hydrogen production. However, an improvement in surface area of TAC was required for enhancing the activity of TAC as catalyst support material.

Keywords: Hydrotalcites, Supported materials, Nickle, Zinc, Hybrid catalysts

1. Introduction

Hydrogen is one of the most promising energy sources as a clean fuel for the future and can be expected to also reduce emissions of greenhouse gases. Biological processes served as alternative routes for hydrogen production due to its environmental benefits from both waste substrate utilization and simple operation. However, hydrogen yields reported in the literatures were lower than the maximum theoretical hydrogen yield of 4 mol H_2/mol glucose, when acetic acid is the end-product [1-2]. In practice, the mixture of the end products such as acetic acid, butyric acid, and lactic acid are produced that cause low hydrogen yields. In addition, the accumulation of soluble acid metabolites in fermentation broth inhibits the process of hydrogen production with a sharp drop in the system pH. Improvements in the bioactivity of hydrogen producing bacteria as well as the avoidance of end-product inhibition are needed to achieve a high yield of hydrogen production. Recently, there has been some

Corresponding Author E-mail: pornthip.wim@sru.ac.th

interest in improving biohydrogen production by catalytic applications, particularly metal catalyst [3-5] and hydrotalcite (HT) [6]. Depended on their unique properties, hydrogen yield increased from 2.30-4.48 mol H_2/mol sucrose. The role of nanocatalysts displayed in distinguished performances. The 5-nm-gold particles were found as electron sinks for hydrogen formation. In addition, activated carbon (AC) can be used to avoid VFA accumulation, particularly butyric acid [7]. Another function is electron transfer by Fe/SiO_2 and Mg-Al HT nanoparticles resulting increase in hydrogen production from 38-64% as compared to the control. However, a single function of nanomaterial is still limited to the yield of hydrogen and application. Thus, improving catalysts activity, selectivity, and stability is essential for progress in the field of fermentative hydrogen production. AC and metal catalysts provide the possibility to modify as multi-functional catalysts. AC can act as simultaneously as an adsorbent and as a support for catalyst [8-9]. It is well known from the literature that highly porous structure and surface chemistry of AC support highly affect the activity of the catalyst [10]. More important, AC as a support material facilitates the reuse of metal catalysts. Besides the function of metal catalyst mentioned above, the base metal catalyst of HT can slow down a decrease of pH and towards favorable metabolic pathways. AC can use to maintain the levels of butyric acid which was below the inhibitory level. Thus, with the unique properties and the combined effect of carbon and metal catalysts, it can be defined as the limiting control pathway in the metabolic resulting in more hydrogen production. The main focus of this study is the development of multi-functional hybrid materials for catalytic applications, particularly for the fermentative hydrogen production process. The morphology properties, the composition of catalysts, and metal active catalysts were studied for the enhancement of fermentative hydrogen production.

2. Experimental details

2.1 Catalyst preparation

Commercial activated carbon (CAC) and treated activated carbon (TAC) were used as metal catalyst supports. TAC obtained from the National Nanotechnology Center, Thailand was chemically treated to obtain a highly porous structure. Prior to use, the CAC and TAC were sieved to a particle size of 1,180 μm. The modified hydrotalcite (HT) with Ni (Ni-HT) and Zn (Zn-HT) catalysts loading on activated carbon support were prepared by the incipient impregnation method. The amount of granular AC at 6 g was impregnated with 6 mL of an aqueous solution containing an appropriate amount of $Mg(NO_3)2{\cdot}6H_2O$, $Al(NO_3)_3{\cdot}9H_2O$, $Ni(NO_3)_2{\cdot}6H_2O$ and $Zn(NO_3)_2{\cdot}6H_2O$. The impregnated support was dried in static air at room temperature for 1 h, followed by drying and at 60 °C for 1 h and at 105°C for 3 h. Then, the material was impregnated with 3 ml of an aqueous solution containing both (2.25 M) NaOH and (0.45 M) Na_2CO_3. The impregnated support was placed in an autoclave. The sample was heated to the desired temperature of 60 °C for 24 h in a water-saturated atmosphere and dried afterward at 60 °C in static air for 4 h. The catalyst precursor was thoroughly washed with demineralized water and dried at 105 °C for 24 h.

2.2 Catalysts characterization

The functional groups of samples were analyzed by Fourier transform infrared (FT-IR) spectra. FT-IR spectra were recorded on a spectrophotometer at ambient temperature using a potassium bromide (KBr) disk method. The spectra were recorded at 2 cm^{-1} resolution with a total of 32 scans with wave numbers ranging from 400 to 4000 cm^{-1}. In addition, the characteristics of carbon - metal active catalysts were examined BET and SEM analysis at the

National Nanotechnology Center, Thailand. The samples were dried in an oven at 60 °C for 2 h before their SEM analysis. The structures of HTs on AC support were analyzed by X-ray powder diffraction (XRD). XRD technique using a Bruker D8 instrument equipped with a Cu target at the National Nanotechnology Center, Thailand. XRD patterns were recorded at 40 kV and 40 mA by using Cu K_α radiation (λ=0.15406 nm) at a rate of 5°/min from 2Θ= 5° to 80°.

2.3 Catalyst activity

Batch tests were carried out in a dark fermentation process to investigate the enhancement of fermentative hydrogen production by using carbon - metal active catalysts. AC and metal catalysts were used separately to estimate the promoting effect of carbon - metal active catalysts on hydrogen production. The catalytic experiments were conducted in a dark fermentation batch. The amounts of catalysts, in the range of 5.00-16.67 g/L, were added into 10 mL of heat-treated sludge and enriched with 45 mL of synthetic medium, together with 5 mL of nutrients solution. These experiments were conducted using the procedure as described in previous studies [6]. The initial pH of 5.5 will be adjusted using 1N NaOH or 1N HCl. The bottles were capped with a butyl rubber stopper, sealed with an aluminum crimp. Anaerobic conditions were created by sparging with nitrogen gas for 3 min. To inhibit the activity of photosynthetic bacteria, the serum bottles were wrapped with aluminum foil. The serum bottles were cultivated in an incubator shaker under the mesophilic condition at 37ºC and shake at 90 rpm. The heat-treated sludge enriched with 60 mL of synthetic medium without any addition of catalysts was used as the control. The amount of evolved gas was measured at room temperature by syringes. The gas compositions were determined by gas chromatograph (GC).

2.4 Determination of biogas composition

The accumulated gas in the head space of the serum bottles was collected using syringes. Before each sampling event, a 60-mL syringe was used to equilibrate the pressure inside the bottle to the ambient pressure, and the volume in the syringe was recorded. The components of biogas (hydrogen and carbon dioxide) were analyzed by a gas chromatograph, GC (PerkinElmer, USA) equipped with a thermal conductivity detector (TCD) and fitted with a Porapak Q, 50/80 mesh column. Helium gas was used as the carrier gas at a flow rate of 25 mL/min. The operating temperatures of the column, detector, and injector were 45, 100, and 100 °C, respectively.

2.5 Kinetic modeling

A modified Gompertz model (Equation 1) was widely used to describe the progress of a batch fermentative hydrogen production process and to establish the relationship among the substrate degradation rate, the hydrogen-producing growth rate, and product formation rate. The hydrogen production data will be fitted to the model to estimate values of parameters.

$$H = H_{max} \exp\{ - \exp[\frac{R_m * e}{H_{max}} (\lambda - t) + 1]\} \quad (1)$$

Where, H and H_{max} denote the cumulative hydrogen production (mL) and the maximum cumulative hydrogen production (mL), respectively. R_m represents the hydrogen production rate (mL/h), and λ, t, and e are the lag-phase time (h), the cultivation time (h), and the Euler's constant (2.718), respectively.

3. Results and discussion

3.1 Effect of activated carbon as HT catalyst supports on hydrogen production

In this study, CAC and TAC with the same particle size of 1.00 mm at a dose of 8.33 g/L were used as catalyst supports of Ni-HT and Zn-HT. The effect of AC on their performance as HT catalyst supports for fermentative hydrogen production were determined. It can be seen from Fig. 1 that CAC with and without active metal catalysts of Ni-HT and Zn-HT showed no significant difference in hydrogen production, while TAC with loading HTs both of Ni-HT/TAC and Zn-HT/TAC catalysts presented a higher amount of hydrogen production of 19.65% and 52.64%, respectively, compared to TAC without loading HTs catalyst. For active metal catalysts, Zn-HT/TAC exhibited a hydrogen production much higher than that obtained from Ni-HT/TAC. The catalytic activity was greatly improved in TAC. This may be due to its relatively large surface area, compared to CAC. Further, understand the difference in properties of activated carbon as HT catalyst supports, the characteristics were examined and reported in the characterization of activated carbon supported modified HT with Ni and Zn catalysts section.

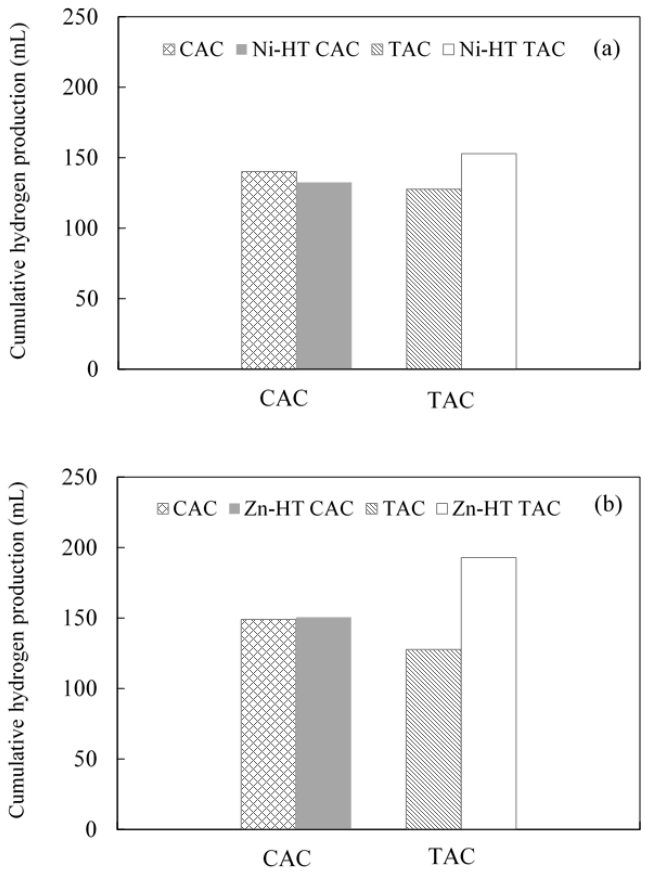

Fig. 1. The maximum cumulative hydrogen production obtained from of CAC and TAC with and without loading Ni-HT (a) and Zn-HT (b)

3.2 Effect of TAC supported HT doses on hydrogen production

The best activity of TAC as HT catalyst supports were selected for further study. The effect of TAC supported HT doses in the range of 5.00-16.67 g/L on hydrogen production was studied. As shown in Fig. 2, Ni-HT/TAC batch was carried out at different doses of 5.00-16.67 g/L and analyzed for their hydrogen production. The addition of Ni-HT/TAC at 8.33 g/L showed a significant difference in hydrogen production over the studied range of 5.00-16.67 g/L during a fermentation time of 360 h (Fig. 2 (a)). The maximum cumulative hydrogen production was 2.3 folds of the control. However, the addition of Ni-HT/TAC at 11.67 and 16.67 g/L showed a lower increment of hydrogen production after 168 h of investigation (Fig. 2 (b)). The reason was probably that the high dose of 11.67 and 16.67 g/L of Ni-HT/TAC showed a strong base property that inhibited the hydrogen production at the final stage.

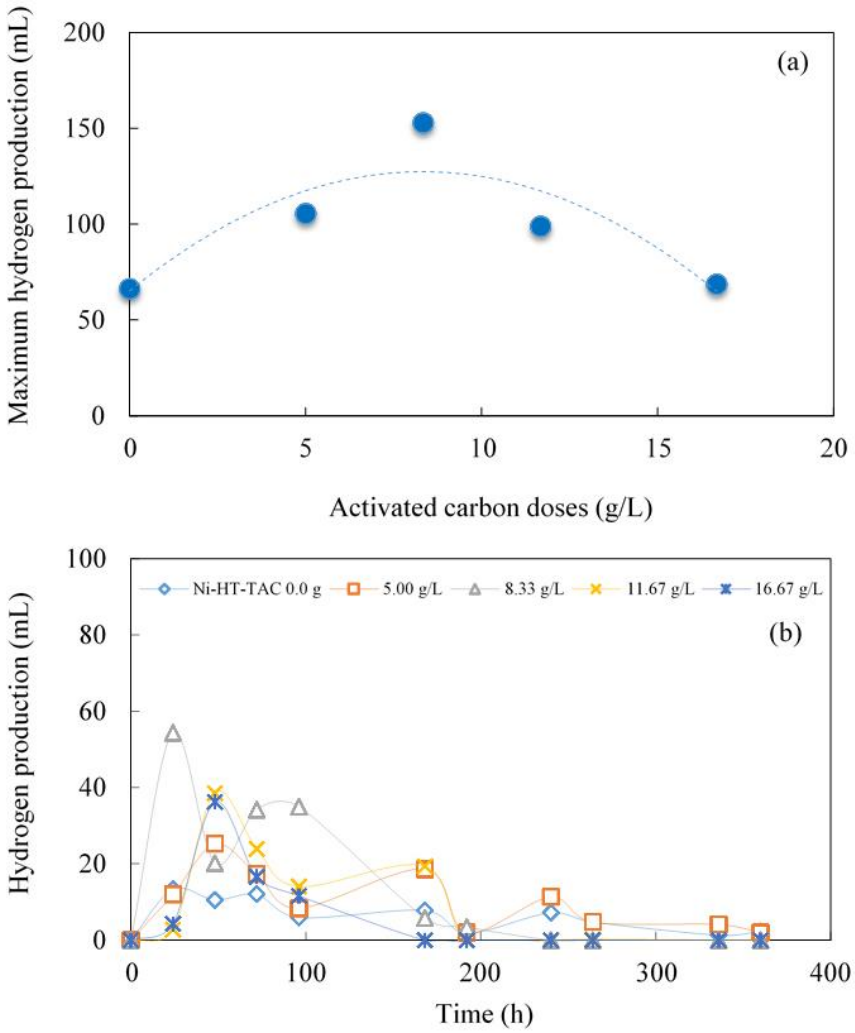

Fig. 2. The maximum cumulative hydrogen production (a) and hydrogen production (b) at different doses of Ni-HT/TAC.

In the case of Zn-HT/TAC, the pattern of hydrogen production at different doses was similar to Ni-HT/TAC batch. A slight increase in hydrogen production was observed over the studied range of 5.00-11.67 g/L as compared to the control. However, the addition of Zn-HT/TAC at 16.67 g/L showed a lower hydrogen production than that of the control (Fig. 3 (a)). The hydrogen production profiles showed that the initial activities of high doses at 11.67 and 16.67 g/L were more active than Zn-HT/TAC at low doses. On the contrary, the activity observed at 5.00 and 8.33 g/L were more stable than Zn-HT/TAC at high doses (Fig. 3 (b)). After 120 h, the high doses tests showed an inhibiting effect with low hydrogen production. In contrast, the addition of lower doses, the reaction remained active and stable even after 216 h of fermentation in an acidic environment. When a system was started with a high rate of hydrogen production, VFAs were produced as by-products, causing a drop in pH in the system. This resulted in low hydrogen production at high doses of Zn-HT/TAC.

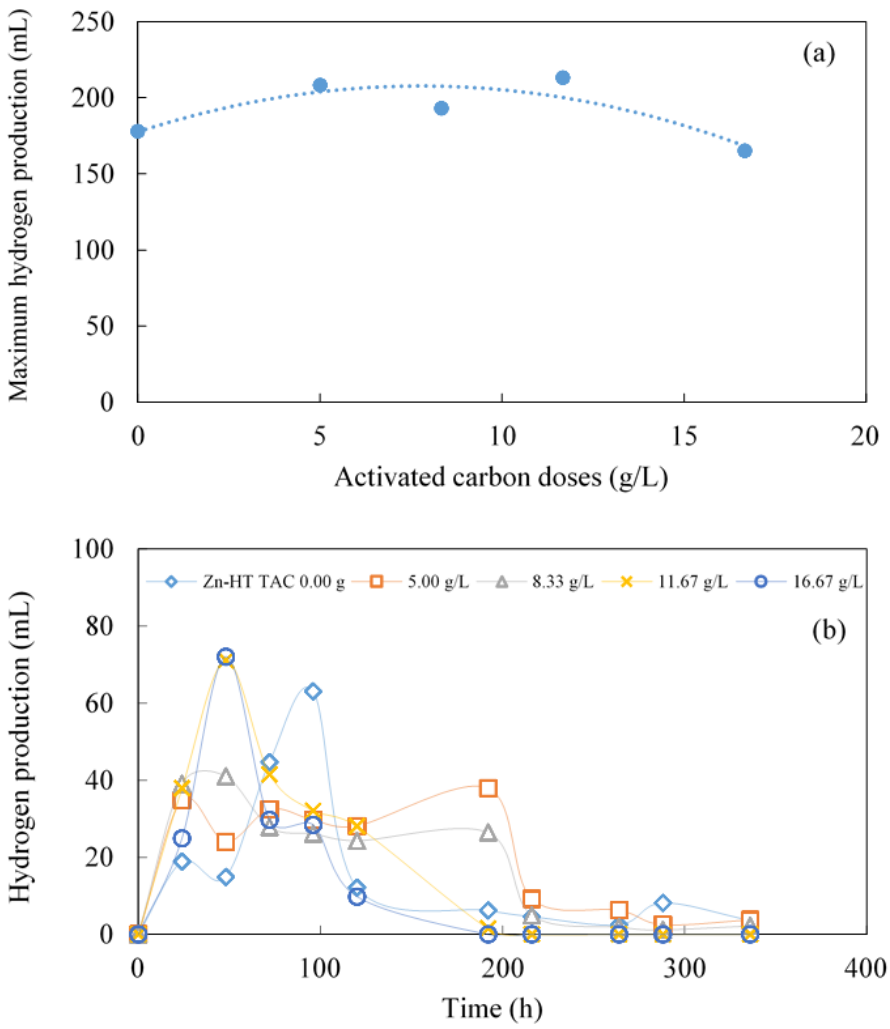

Fig. 3. The maximum cumulative hydrogen production (a) and hydrogen production (b) at different doses of Zn-HT/TAC.

3.3 Comparison of TAC supported modified HT with Ni and Zn catalysts on hydrogen production

The catalysts consisting of TAC, Ni-HT/TAC, and Zn-HT/TAC were determined at the optimum dose of 8.33 g/L. The hydrogen production profiles showed that the initial activity of Ni-HT/TAC and Zn-HT/TAC at 24 h was more active than a single TAC catalyst (Fig. 4). On the contrary, after 48 h, the activity of a single TAC catalyst was more active than Ni-HT/TAC. Under the combination of catalysts condition of TAC supported modified HT with Ni and Zn catalysts, the activity takes place faster and produces the hydrogen production at a higher rate. However, a high rate of hydrogen production accompanied by VFAs as a byproduct that resulted in the accumulation of acetic acid, butyric acid, and lactic acid in the system. This phenomenon was an undesirable condition and reduced the term of the hydrogen fermentation process. The addition of the Zn catalyst resulted in a positive increment of hydrogen production after 120 h as compared to TAC. The pattern of hydrogen production was similar for all catalysts with decreasing activity after 96 h.

The maximum cumulative hydrogen production and hydrogen production rate were reported in Fig. 5. All catalyst tests showed an improvement in hydrogen production. The cumulative hydrogen productions obtained for difference catalysts were fitted with the modified Gompertz Equation as described in Equation (1). The result showed that the catalysts of Ni-HT/TAC in fermentation broth resulted in lower hydrogen production than that obtained from a single catalyst of TAC during a fermentation period of 300 h. With the addition of TAC, a higher increment of the maximum cumulative hydrogen production of 17.75% was observed as compared to control. However, an increase in the hydrogen production rate was obtained from the catalysts of Ni-HT/TAC. The maximum cumulative hydrogen production was obtained from Zn-HT/TAC and Ni-HT/TAC with 26.62% and 9.29% increment as compared to the control, respectively. The comparison was carried out in terms of hydrogen production over two active metal of Ni and Zn catalysts. Ni-HT/TAC was more active than that obtained from Zn-HT/TAC catalysts during the initial stage of 24 h. This is due to the fact that the basic sites of on Ni-HT catalyst were related to the rapid decomposition of saccharides [11]. In addition, It is suspected that the presence of Ni^{2+} and NiO was associated with the higher activity of hydrogenase caused the shift of metabolic pathways towards more efficient hydrogen fermentation [12-15]. However, a catalyst of Zn-HT/TAC showed was more stable than Ni-HT/TAC. This is due to the fact that the addition of HT containing Zn provided the active sites of hydrogenase enzyme which facilitates area for reaction and then improved activity [16]. In the case of Zn-HT/TAC, the base property slowly released and slow down a decrease of pH from 5.5 to 4.17 at the end fermentation. However, the final pH value of Zn-HT/TAC was higher as compared to Ni-HT/TAC at a pH of 4.04. To further study the effect of hybrid catalysts, the characterization of HT and activated carbon was explained in the next section.

Table 1 presents the hydrogen yield obtained from batch tests using different catalyst materials. Catalyst activities included facilitating high area for reaction, a shift of metabolic pathways, constructive outcomes of action on the hydrogenases, immobilization carrier addition, and solid base catalysts toward more efficient hydrogen fermentation. The maximum hydrogen yield obtained in this study was higher than that of single metal catalysts of Gou et al., 2015 [17] and Wimonsong et al, 2013 [6]. However, in comparison to other studies, as indicated in Table 1, the Ni-HT/TAC catalysts used this study has a slight enhancement of hydrogen production in relation to the control.

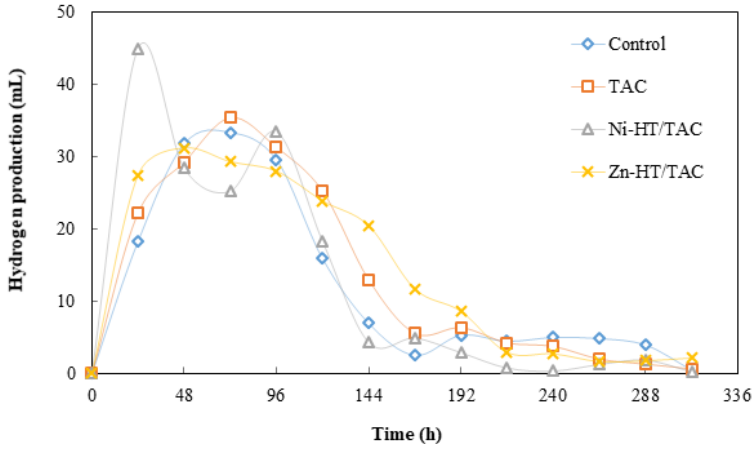

Fig. 4. The hydrogen production at different doses of Ni-HT/TAC difference catalysts combination

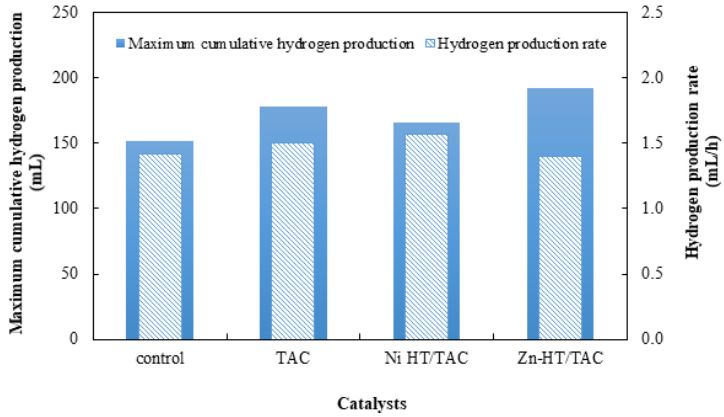

Fig. 5. The maximum cumulative hydrogen production using difference catalysts combination.

Table 1. Hydrogen yields obtained from batch tests using different catalyst materials

Type	Activity	H_2 yield	% increment in relation to control	Ref.
Ni nanoparticles	Facilitates high area for reaction	2.54[b]	23.00	[18]
Ni^{2+}	shift of metabolic pathways	2.05[a]	107.10	[19]
Zn-Mg-Al HT	New active sites for enzyme	2.10[a]	31.30	[6]
Fe^0 and Ni^0	the fundamentals for the development of microbes	147.30[d]	200.00	[20]
Zero-valent iron, activated carbon	Constructive outcomes of action on the hydrogenases	429.00[c]	50.20	[21]
Activated carbon	Immobilization carrier addition	1.20[b]	2.94 (times)	[22]
Ni-HT/TAC	Basicity property	2.66[a]	9.29	This study
Zn-HT/TAC	Basicity property	3.08[a]	26.62	This study

Note: [a]mol H_2/mol sucrose, [b]mol H_2/mol glucose, [c]mL/g glucose, [d]mL/g-starch

3.4 Characterization of TAC supported modified HT with Ni and Zn catalysts

To further understand the properties of TAC supported modified HT with Ni and Zn catalysts, FTIR were examined. For all of the samples, a broad band in the 3460 cm^{-1} was assigned to the O-H stretching mode band in water (Fig.6). A broad band at 1566 cm^{-1} can be allocated to C=C aromatic ring stretching vibration enhanced by polar functional groups. The peak at 1384 cm^{-1} indicates the presence of the carbonate anion in the interlayer region of the HT. The bands in the region between 1084.22 cm^{-1} and 800 cm^{-1} were assigned to C-O stretching in acids, alcohols, phenols, ethers, and esters, usually found in oxidized carbons. In the TAC supported modified HT sample containing Zn^{2+}, the peaks in the region 400-800 cm^{-1} are assigned to the stretching mode of metal oxide.

The structures of Ni-HT and Zn-HT on TAC support were analyzed by XRD. As can be seen from Fig.7, XRD patterns of the Ni-HT/TAC and Zn-HT/TAC can be attributed to a typical hydrotalcite structure. The peak at the two theta degree of 23° corresponds to carbon support [23]. For the Ni-HT/TAC catalyst, the peaks at the two theta degrees of 44° and 77° are ascribed to (111) and (220) lattice planes of the metal Ni and the peak of 37.2° and 62.5° are indexed to NiO (111) and NiO (220) [8]. In case of Zn-HT/TAC, the peaks at the two theta degrees of 43°, 57°, and 74° are corresponds to Zn and the peaks at the two theta degrees of 31.7°, 34.4°, and 36.2° corresponding to the diffraction planes of (100), (002), and (101) respectively, confirm the structure of ZnO particles [24]. The XRD patterns exhibit the characteristic diffractions of HT, indicating that the modified hydrotalcite with Ni and Zn were successfully coated onto TAC by the incipient impregnation method.

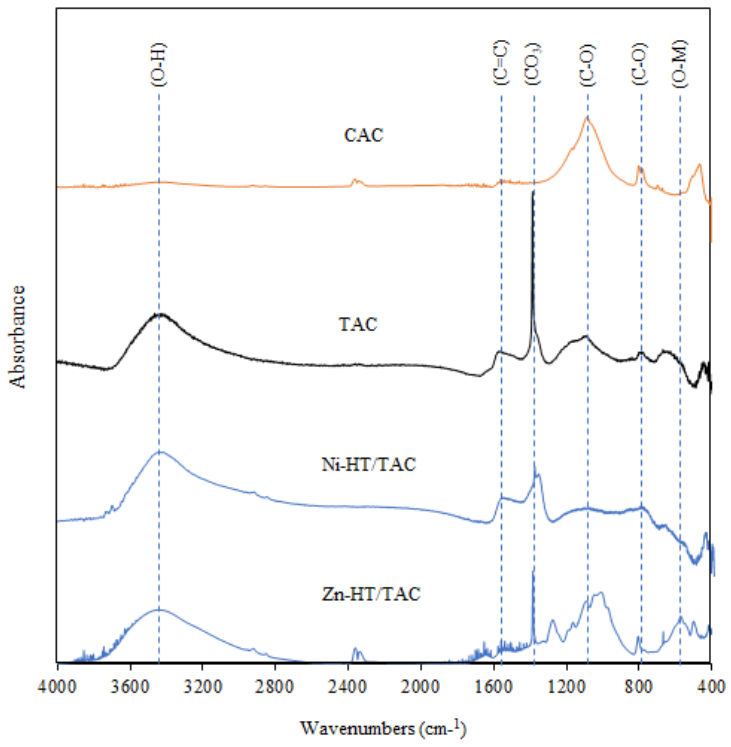

Fig. 6. FTIR spectra of CAC, TAC, Ni-HT/TAC and Zn-HT/TAC

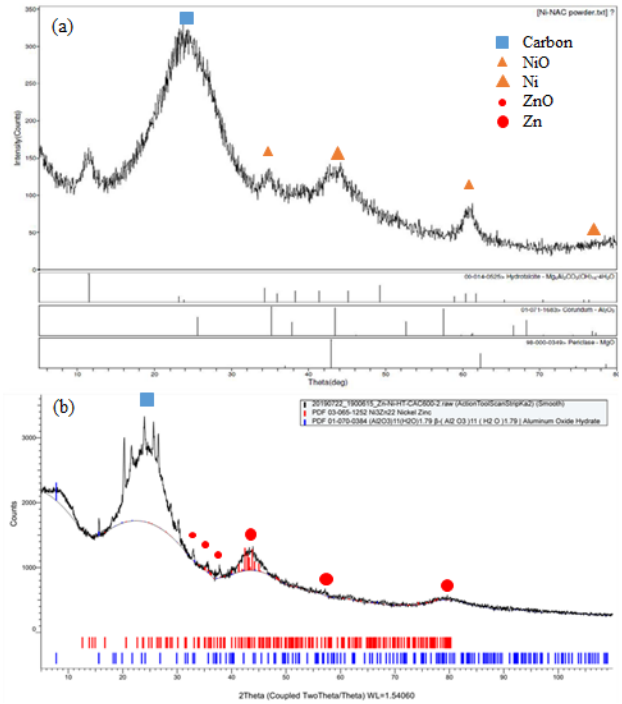

Fig. 7. XRD pattern of Ni-HT/TAC (a) and Zn-HT/TAC (b)

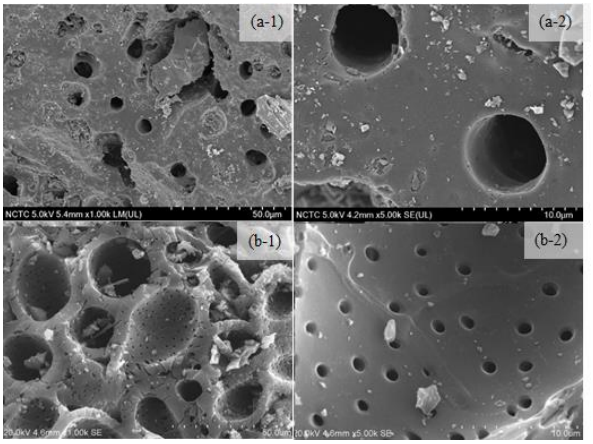

Fig. 8. Scanning electron micrograph of CAC (a) and TAC (b) at different magnification of 50 (1) and 10 (2) µm

The surface morphology of activated carbon is shown in the SEM micrograph (Fig. 8). CAC showed less surface roughness with larger pore size (Fig.8 (a-1) and (a-2)) as compared to TAC (Fig.8 (b-1) and (b-2)). The BET surface area and total pore volume of TAC were reported at 1,129.45 m^2/g and 0.48 cm^3/g, respectively which was much higher as compared to CAC (Table 4). TAC was activated to obtain greater active sites and areas which could beneficial to fermentative hydrogen production.

A highly porous surface area of TAC supported Ni-HT and Zn-HT were evidenced through the SEM images. As can be seen in Fig. 9, TAC exhibited irregular surfaces with pores of different shapes and sizes. The SEM images of TAC- supported Ni-HT and Zn-HT revealed that the Ni-HT and Zn-HT were deposited on the TAC surfaces. In addition, BET analysis was studied as shown in Table 2. The BET surface area of Ni-HT/TAC and Zn-HT/TAC were reported at 702.90 $m^2 \cdot g^{-1}$ and 868.10 $m^2 \cdot g^{-1}$ and total pore volume of 0.31 $cm^3 \cdot g^{-1}$ and 0.37 $cm^3 \cdot g^{-1}$ respectively which was lower than that of TAC without HT loading. This is possible that TAC support generally leads to a decreased surface area after loading metal catalyst.

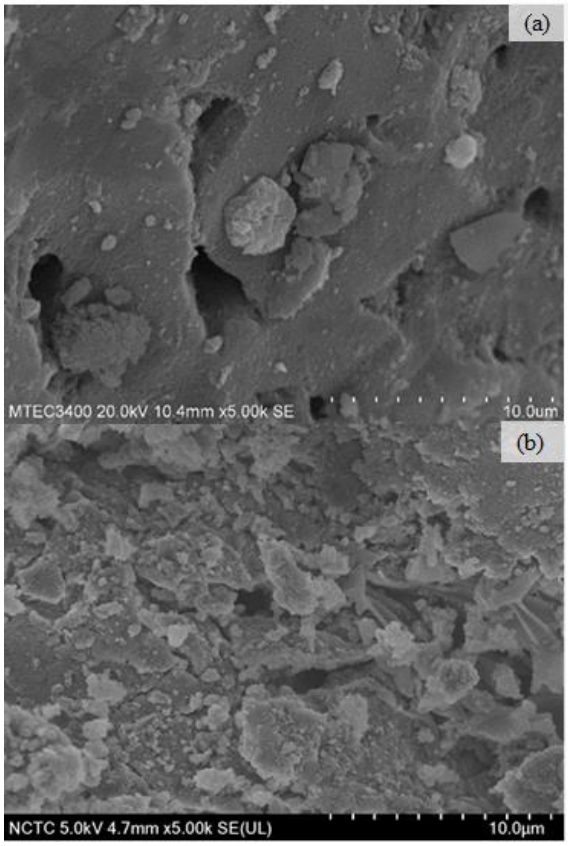

Fig. 9. Scanning electron micrograph of Ni-HT/TAC (a) and Zn-HT/TAC (b) at magnification of 10 µm

Table 2. Physical properties of different material

Catalysts	Specific Surface Area (m^2/g)	Total Pore Volume (cm^3/g)
CAC	761.00	0.37
TAC	1129.45	0.48
Ni-HT/TAC	702.90	0.31
Zn-HT/TAC	868.10	0.37

As can be seen in Table 2, specific surface area and total pore volume of TAC was higher than CAC. However, after loading modified HT with Ni and Zn, specific surface area and total pore volume of hybrid catalysts were lower than that obtained from TAC without loading metal HT. Therefore, the impregnation of TAC with the HT resulted in changes in specific surface area and total pore volume with a decrease of 37.76% and 23.14% for Ni-HT and Zn-HT, respectively. HT was formed leading to blockage of some micropores and mesopores. The activation process which showed an increase in specific surface area was required for enhancing the activity of support material.

4. Conclusion

In conclusion, TAC supported modified HT with Ni and Zn catalysts were applied in fermentative hydrogen production. The characterization of TAC supported exhibit that the modified hydrotalcite with Ni and Zn were successfully coated onto TAC by the incipient impregnation method. The results show that the catalytic activity was improved in TAC due to its relatively large surface area, compared to CAC. However, the decrease in specific surface area and total pore volume of TAC were observed after loading modified HT with Ni and Zn. Therefore, the impregnation of TAC with the metal HT resulted in a decrease in specific surface area and total pore volume, especially Ni-HT/TAC. The comparison was carried out in terms of hydrogen production over two active metal of Ni and Zn catalysts. Ni-HT/TAC was more active than that obtained from Zn-HT/TAC catalysts during the initial stage of 24 h due to the rapid decomposition of Ni-HT catalyst. However, a catalyst of Zn-HT/TAC showed was more stable than Ni-HT/TAC during the final stage due to a slow release of the base property. The maximum cumulative hydrogen production was obtained from Zn-HT/TAC with 26.62% and 7.53% increment as compared to the control and TAC, respectively. On the other hand, Ni-HT/TAC showed a decrease in the maximum cumulative hydrogen production with 7.18% as compared to TAC. Therefore, TAC can be used as alternative support material for Zn-HT catalysts. However, an improvement in surface area of TAC was proposed to achieve higher efficiency and stability for enhancing the activity of support material.

Acknowledgment

The authors gratefully acknowledge the financial support provided by The Thailand Research Fund Grant for New Researcher, Contract No. MRG5980105.

References

[1] Sharma Y, Li B. Optimizing hydrogen production from organic wastewater treatment in batch reactors through experimental and kinetic analysis. Int J Hydrogen Energy. 2009;34: 6171-80.

[2] Prasertsan P, O-Thong S, Birkeland NK. Optimization and microbial community analysis for production of biohydrogen from palm oil mill effluent by thermophilic fermentative process. Int J Hydrogen Energy. 2009;34:7448-59.

[3] Han H, Cui M, Wei L, Yang H, Shen J. Enhancement effect of hematite nanoparticles on fermentative hydrogen production. Bioresour Technol. 2011;102:7903-9.

[4] Zhang Y, Shen J. Enhancement effect of gold nanoparticles on bio-hydrogen production from artificial wastewater. Int J Hydrogen Energy. 2007;32:17-23.

[5] Zhao W, Zhao J, Chen G, Feng R, Yang J, Zhao Y, Wei Q, Du B, Zhang Y. Anaerobic biohydrogen production by the mixed culture with mesoporous Fe_3O_4 nanoparticles activation, Adv Mat Res. 2011;306-307:1528-31.
[6] Wimonsong P, Llorca J, Nitisoravut R. Catalytic activity and characterization of Fe-Zn-Mg-Al hydrotalcites in biohydrogen production. Int J Hydrogen Energy. 2013;38: 10284-92.
[7] Wimonsong P, Nitisoravut R. Biohydrogen enhancement using highly-porous activated carbon. Energy & Fuels. 2014;28(7):4554-9.
[8] Lei H, Yang L, Shengtao W, Pingle L, Wei X, Fang H, He'an L. Activated carbon supported bimetallic catalysts with combined catalytic effects for aromatic nitro compounds hydrogenation under mild conditions. Applied Catalysis A, General. 2019;577:76–85.
[9] László V, Ádám P, EmÅke S, Edina R, Gábor M, Ferenc K, Béla V, Béla F. Application of carbon nanotube coated aluminosilicate beads as "support on support" catalyst for hydrogenation of nitrobenzene. J Ind Eng Chem. 2019;79:307-13
[10] Meryemoglu B, Irmak S, Hesenov A, Erbatur O. Preparation of activated carbon supported Pt catalysts and optimization of their catalytic activities for hydrogen gas production from the hydrothermal treatment of biomass derived compounds. Int J Hydrogen Energy. 2012;37:17844-52.
[11] Willinton YH, Jeroen L, Pascal Van Der Voort, An V. Recent advances on the utilization of layered double hydroxides (LDHs) and related heterogeneous catalysts in a lignocellulosic-feedstock biorefinery scheme. Green Chemistry. 2017;19:5259-16.
[12] Elreedy A, Ibrahim E, Hassan N, El-Dissouky A, Fujii M, Yoshimura C, Tawfik A. Nickel-graphene nanocomposite as a novel supplement for enhancement of biohydrogen production from industrial wastewater containing mono-ethylene glycol. Energy Convers Manag. 2017;140:133–44.
[13] Wang JL, Wan W. Influence of Ni^{2+} concentration on biohydrogen production. Bioresour Technol. 2008;99:8864–8.
[14] Mishra P, Thakur S, Mahapatra DM, Ab Wahid Z, Liu H, Singh L. Impacts of nanometal oxides on hydrogen production in anaerobic digestion of palm oil mill effluent-A novel approach. Int J Hydrogen Energy. 2018;43:2666-76.
[15] Gadhe A, Sonawane SS, Varma MN. Enhancement effect of hematite and nickel nanoparticles on biohydrogen production from dairy wastewater. Int J Hydrogen Energy. 2015;40:4502-11.
[16] Wimonsong P, Nitisoravut R, Llorca J. Application of Fe-Zn-Mg-Al-O hydrotalcites supported Au as active nano-catalyst for fermentative hydrogen production. Chem Eng J. 2014;253:148-54.
[17] Guo L, Li XM, Bo X, Yang Q, Zeng GM, Liao D, Liu JJ. Impacts of sterilization, microwave and ultrasonication pretreatment on hydrogen producing using waste sludge. Bioresour Technol. 2008:99(9);3651-8.
[18] Mullai P, Yogeswari MK, Sridevi K. Optimisation and enhancement of biohydrogen production using nickel nanoparticles-A novel approach. Bioresour Technol. 2013;141:212-9.
[19] Gou CY, Guo JB, Lian J, Guo YK, Jiang ZS, Yue L, Yang JL. Characteristics and kinetics of biohydrogen production with Ni^{2+} using hydrogen-producing bacteria. Int J Hydrogen Energy. 2015;40:161–7.
[20] Taherdanak M, Zilouei H, Karimi K. Investigating the effects of iron and nickel nanoparticles on dark hydrogen fermentation from starch using central composite design. Int J Hydrogen Energy. 2015;40:12956-63.

[21] Zhang L, Zhang L, Li D. Enhanced dark fermentative hydrogen production by zero-valent iron activated carbon micro-electrolysis. Int J Hydrogen Energy. 2015;40: 12201-8.
[22] Zhang CS, Kang XX, Liang NN, Abdullah A. Improvement of biohydrogen production from dark fermentation by cocultures and activated carbon immobilization. Energy Fuels. 201731:12217–22.
[23] Kobayashi H, Matsuhashi H, Komanoya T, Hara K, Fukuoka A. Transfer hydrogenation of cellulose to sugar alcohols over supported ruthenium catalysts. Chem Commun. 2011; 47:2366-8.
[24] Vinayagam M, Saranya R, Ramya V, Sivasamy A. Photocatalytic degradation of orange G dye using ZnO/biomass activated carbon nanocomposite. J Environ Chem Eng. 2018; 6(3): 3726-34.